Malaysian Journal of Chemistry, 2024, Vol. 26(5), 387-396
(Special Issue: *4th IKMPB Online Symposium 2024 - Development of Chemistry to Accomplish a Sustainable World*)

Adsorption Kinetic, Isotherm and Mechanism Study of Xanthate-Modified Neem Leaf Powder as an Efficient Adsorbent for Methylene Blue Dye

Mardhiah Ismail*, Shaari Daud, Zul Adlan Mohd Hir, Sabarina Md Yunus and Megat Ahmad Kamal Megat Hanafiah
Faculty of Applied Sciences, Universiti Teknologi MARA Pahang, 26400 Bandar Tun Abdul Razak Jengka, Pahang, Malaysia
*Corresponding author (e-mail: marismael@uitm.edu.my)

This research investigates the behaviour of a xanthate-modified neem leaf powder (XNL) in removing methylene blue (MB) from an aqueous solution. Different treatments will create different unique characteristics of adsorbent. At the same time, each specific treated adsorbent will behave differently with different adsorbates. XNL is proven as an efficient and low-cost adsorbent for removing methylene blue (MB) dye from an aqueous solution. Fourier Transform Infra-red (FTIR), Thermogravimetric (TGA), Energy Dispersive X-ray spectroscopy (EDX), and Brunauer–Emmett–Teller (BET) were used to investigate the properties of XNL. These characterisations suggest that XNL has a specific area of 6.02 $m^2 g^{-1}$. The influence of adsorption parameters such as adsorbent dosage, solution pH, contact time, and initial MB concentrations was studied, and it was found that the optimum condition for MB adsorption is at pH 6 with the adsorbent dosage of 0.02 g. The adsorption results were well described by pseudo-second-order (PSO) kinetic, and adsorption isotherm, followed by both Langmuir and Freundlich models. The maximum adsorption capacity (q_{max}) of XNL for MB dye was found to be 263.80 mg g^{-1} at 318 K. Thus; this work indicates that the XNL can be used as a promising adsorbent for MB dye from aqueous solution. The MB dye adsorption mechanism by XNL can be assigned to several types of interactions, such as electrostatic attractions, H-bonding interaction, and n-π interaction.

Keywords: ***A****zadirachta*; isotherm; kinetic; neem; xanthate

Received: January 2024; Accepted: July 2024

Water pollution remains one of our most critical environmental challenges, with synthetic dyes posing a significant threat to aquatic ecosystems and human health. Methylene blue is notably prevalent among these dyes due to its extensive use in various industries, including textiles, paper, printing and medical diagnostics [1]. Methylene blue, a cationic dye, poses significant environmental hazards due to its persistence and potential toxicity. Despite its utility, the improper discharge of methylene blue into water bodies leads to severe environmental consequences, necessitating effective remediation strategies. Methylene blue, a cationic thiazine dye, is known for its high visibility and potential toxicity, even at low concentrations. Its presence in aquatic environments can impede photosynthetic processes by reducing light penetration and disrupting the ecological balance [2]. Moreover, methylene blue is resistant to biodegradation, leading to persistent contamination and bioaccumulation, which pose long-term risks to both aquatic life and human health, including vomiting, high heart rate, nausea, tissue necrosis, jaundice and quadriplegia [3]. Adsorption has emerged as a promising treatment method to mitigate the adverse effects of methylene blue pollution [4]. This technique offers several advantages, including high efficiency, cost-effectiveness, and the ability to target a wide range of contaminants [5]. Adsorption emerges as a viable and sustainable approach for removing MB from contaminated water sources [6-7]. Recent research has focused on developing novel adsorbents with enhanced capacity and selectivity for methylene blue, utilising materials such as activated carbon, natural clays, and various nanocomposites. Among the numerous adsorbents investigated for pollutant removal, neem leaf powder emerges as a promising candidate due to its abundant availability, cost-effectiveness, and eco-friendly nature. This study delves into the adsorption of MB, a commonly encountered dye pollutant, onto xanthate-treated neem leaf powder, aiming to elucidate its efficacy and mechanisms [8-9]. Removing MB from aqueous solutions is imperative to mitigate its adverse impacts on aquatic ecosystems and human health. Neem (*Azadirachta indica*) leaves, abundant in bioactive compounds with diverse properties, have garnered attention as a potential adsorbent owing to their natural abundance, renewability, and non-toxicity. Xanthate modification of neem leaf powder enhances its surface properties, thereby improving its adsorption capacity towards target pollutants like MB. Xanthates, derived from carbon disulphide, introduce sulphur-

†Paper presented at the 4th IKMPB Online Symposium 2024 – Development of Chemistry to Accomplish a Sustainable World

containing functional groups onto the surface of neem leaf powder, facilitating stronger interactions with MB molecules [10-11]. This study draws inspiration from previous research endeavours that have explored the adsorption potential of neem-based materials for various contaminants. Notably, incorporating xanthate groups onto neem leaf powder presents a novel approach to enhance its adsorption efficiency, paving the way for innovative solutions in wastewater treatment and environmental remediation. The objectives of this study encompass elucidating the adsorption kinetics and adsorption mechanism governing the interaction between MB and xanthate-treated neem leaf powder. Understanding these fundamental aspects is crucial for optimizing the design and implementation of neem-based adsorbents in practical applications. A comprehensive review of the relevant literature provides insights into the adsorption process's mechanism, highlighting the intricate interplay between surface chemistry, solution conditions, and molecular interactions. By integrating theoretical frameworks with experimental observations, this study endeavours to unravel the complexities inherent in the adsorption of MB onto xanthate-modified neem leaf powder [12].

Experimental methodologies employed in this study adhere to rigorous standards, ensuring reproducibility and reliability of results. Batch adsorption experiments are conducted under controlled conditions to investigate the influence of key parameters such as pH, dosage, initial MB concentration, contact time, and temperature on the adsorption process. Characterisation techniques, including TGA and Brunauer-Emmett-Teller (BET) surface area analysis, provide valuable insights into the structural and morphological properties of the adsorbent material. [13]. The findings of this study are anticipated to contribute significantly to the body of knowledge surrounding neem-based adsorbents and their potential applications in wastewater treatment and environmental remediation. Insights gained from the elucidation of adsorption mechanisms and optimisation of process parameters hold promise for the development of sustainable solutions to mitigate water pollution and safeguard public health. The adsorption of methylene blue onto xanthate-modified neem leaf powder represents a promising avenue for pollutant removal, leveraging the unique properties of natural materials for environmental sustainability. This research endeavours to advance our understanding of adsorption phenomena and pave the way for innovative approaches in water treatment and pollution control.

EXPERIMENTAL

Material

Fresh matured neem leaves were collected from Besut, Malaysia. The leaves were separated from the stem and washed to remove soluble impurities before rinsing with deionised water (Water purification system (Type I - 18 mΩ) – Millipore, Elix 5, Germany). The leaves were dried in an oven (Memmert, Germany) at 333 K overnight before being ground by using a mechanical grinder (Grinder, Thomas Wiley, UK) and sieved (Sieve, Retsch GmbH, Germany) to obtain a particle size of 125-250 µm. Dried neem leaf powder was boiled in deionised water for 30 min to destroy microbes, then washed and dried in an oven overnight at 333 K. Methylene Blue (MB) dye (MW: 319.86 g/mol, assay: ~ 88%, λ_{max} = 664 nm) was purchased from QRec (Malaysia). The other reagents utilised throughout this study were analytical grade. All experiments of this research were performed using deionised water.

XNL Preparation

Xanthate treatment was performed using the modified method from Torres-Blancas et al., (2013)[14]. A weight of 10 g boiled neem leaf powder (BNL) was stirred for 2 h in 200 mL of 4 M NaOH solution which can help to liberate new adsorption sites through elimination of pectin, lignin and cellulose. As little as 1 mL carbon disulphide was added into the mixture and was left to stir for another 2 h. The mixture was filtered and washed thoroughly with 500 mL of deionised water. The treated adsorbent was dried in the oven at 333 K overnight and again was grounded and sieved to obtain a homogeneous particle size of 125-250 µm to ensure the stability of adsorption. This xanthate-treated neem leaves (XNL) powder was kept in an airtight container before use.

XNL Characterization

XNL was characterised by a few characterisation methods. The functional group's presence on the XNL surface was determined using a Fourier Transform infrared (FTIR) spectrometer (Spectrum 100, Perkin Elmer, USA) by scanning the sample KBr disc in the range of 450-4000 cm^{-1}. The KBr disc was prepared by mixing a fine ground of 2 mg adsorbent with 200 mg KBr powder. The mass loss of adsorbent as a function of temperature was determined by a thermal gravimetric analyser or TGA (Perkin Elmer, Pyris 1, USA). The Scanning Electron Microscope (FESEM), (Supra 400, Carl Zeiss SMT, Germany) 104 coupled with Electron Dispersive X-RAY (EDX), (Microanalysis, Oxford instrument, 105 UK) was used to analyse the surface morphology of the XNL. The BET surface area and average pore diameter of XNL were determined from a plot of an N_2 adsorption-desorption curve at a 77 K BET analyser (Thermo Scientific, Surfer, Italy). The determination of the pH of zero-point charge (pH_{ZPC}) of the adsorbent was performed according to the method reported [15].

Batch Adsorption Experiments

MB, a basic and cationic dye, has a chemical formula of $C_{16}H_{18}N_3S^+Cl^-$ and a molecular weight of 319.5 g mol^{-1}. MB powder of analytical reagent grade (QRec, Malaysia) was used to prepare a 1000 mg L^{-1} of

MB solution. Dilute solutions of required MB concentrations were successively prepared for batch adsorption experiments. Batch experiments were carried out by mixing 0.02 g of XNL powder with 50 mL MB solution of fixed concentration in 100 mL conical flasks for a specific period. All experiments were done at pH 6 (optimum pH). After the experiment, the sample was centrifuged at 5000 rpm for 5 min to separate XNL from the solution. The amount of MB in the residual solution was analysed by using a UV-visible spectrophotometer (UV-1800, Shimadzu, Japan) at λ_{max} of 664 nm. All experiments were performed in triplicates, and the results were reported as average with RSD < 5%. The amount of MB adsorbed, q_e (mg g^{-1}) was calculated by using Eq. (1), while the percentage of removal of MB was calculated using Eq. (2):

$$q_e = \frac{C_o - C_e}{m} V \quad (1)$$

$$\% \, Removal = \frac{C_o - C_e}{C_o} 100 \quad (2)$$

Where, C_o and C_e are MB concentrations (mg L^{-1}) before and after adsorption, respectively; V is the volume of MB solution (L), and m is the weight of the adsorbent (g). The kinetic study was conducted using different concentrations of MB solutions (20, 30 and 40 mg L^{-1}), and the mixtures were stirred at different time intervals from 0 to 360 min. The data were analysed by using the PFO and PSO models. The isotherm study was carried out with varied concentrations of MB solution (20, 30, 40, 100, 150, 200, 300 and 400 mg L^{-1}) at 298, 308 and 318 K, respectively. The data obtained were analysed by using Langmuir, Freundlich and Dubinin-Reduskevich.

RESULTS AND DISCUSSION

Characteristic of XNL

The functional group present on the surface of XNL and confirmation of adsorption of MB onto XNL can be accomplished by FTIR spectra shown in Figure 1. The peak at 710 cm^{-1}, 1098 cm^{-1} and 1149 cm^{-1} can prove the presence of C-S bond, C=S stretching, and C-O-C stretching of di-thiocarbonyl respectively, in XNL. The possible interaction between XNL-MB is through the exchanging of light metal ions of carboxylate salt with MB by forming electrostatic attraction between negative carboxylate and the positive site of sulphur in MB, which can be confirmed by a shift of carboxylate peak at 1622 to 1607 cm^{-1}. There is also a possible van der Wall force between the polar-induced dipole of C=O of the ester with the positive charge of sulphur in MB, which can be confirmed with a shift in peak from 1404 to 1490 cm^{-1}. It was suggested that MB ion could also attached to XNL through other mechanisms (Figure 1 (bottom)) including hydrogen bonding, n- π, π- π, electrostatic forces and Van der Waals interaction.

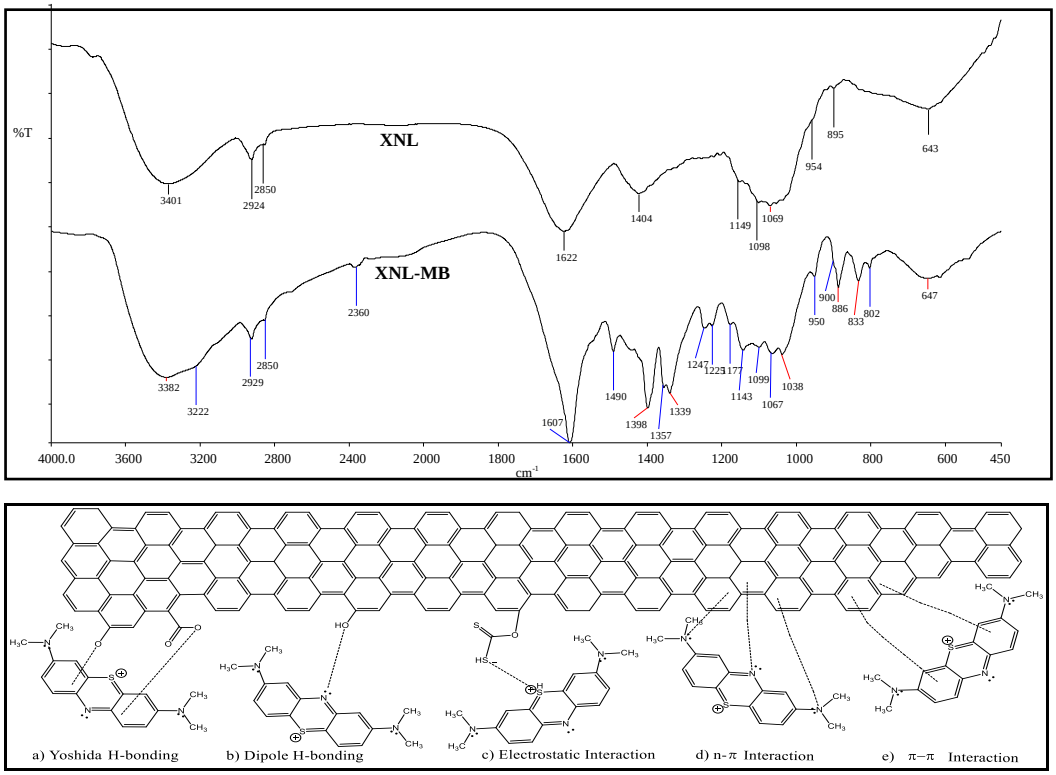

Figure 1 (above) XNL Spectra of XNL and XNL-MB loaded. **(bottom)** Proposed schematic diagram of MB adsorption mechanism (a) Yoshida H-bonding; (b) Dipole H-bonding; (c) Electrostatic Interaction; (d) n-π Interaction and (e) π-π Interaction

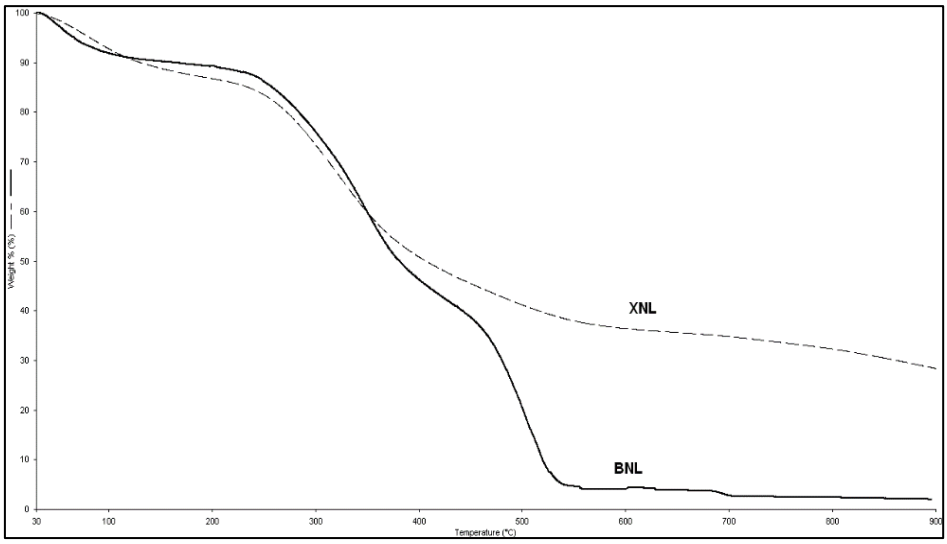

Figure 2. TGA Profile of BNL and XNL.

Thermogravimetric analysis was performed to determine the thermal degradation of cellulose, hemicellulose and lignin in XNL. Figure 2 pictures the weight loss profile and decomposition of XNL against the temperature. The loss of moisture and volatile organic matter that happened in the first 250 °C can be observed in the TGA profile of samples that reduced about 10% to 15% of their mass. Then followed by the loss of hemicellulose and cellulose. Then, it is followed by the long tail that corresponds to the thermal decomposition of lignin. XNL revealed higher weight loss between 250 °C to 550 °C. The loss corresponded to the decomposition of hemicellulose and some portion of cellulose and lignin. The long tail from 550 °C to 900 °C was due to degradation of the remaining cellulose and lignin. Due to high structure stability in XNL, lignin started to decompose at relatively higher temperatures. TGA analysis depicted that the major components of these bio-sorbents were hemicellulose and lignin. Hemicellulose was the easiest to degrade, followed by cellulose. The most stable of all three was lignin, which was the last to degrade. [16].

As reported in Table 1, XNL has a small BET surface area with a pore size of 6.02 m^2 g^{-1}. The xanthation process shrinks the neem leaf powder surface. This finding is similar to the de-oiled allspice husk that decreased the surface pore size after xanthate treatment. [14]. The same finding was also observed after xanthate treatment of insoluble straw, which was found to be smaller than alkali-treated straw [17]. Meanwhile, the Langmuir surface area was 76.19 m^2 g^{-1}, and the pore diameter of XNL was 2.73 nm. Overall, as can be concluded, the pore size of XNL was in the range of mesopores according to the IUPAC scheme or inter-nanopore according to the new pore size classification [18].

Table 1. XNL Properties Before and After Xanthate Modification.

	BNL	**XNL**
pH_{Slurry}	7.15	6.91
pH_{ZPC}	7.18	6.70
S_{BET}[b] (m^2 g^{-1})	11.34	6.02
SL[c] (m^2 g^{-1})	98.14	76.19
DP[d] (nm)	2.71	2.73

Effect of XNL Dosage

The influence of XNL dosage on the removal of MB dye was tested by varying the adsorbent dosage from 0.01 g to 0.02 g, while the other adsorption parameters such as solution volume, initial concentration of MB dye, solution pH, temperature, contact time, shaking speed were kept constant at 50 mL and 20 mg L^{-1}, 6, 298 K, 300 min, and 480 rpm, respectively. As shown in Figure 3a., the amount of XNL increased from 0.01 to 0.02 g, and the percentage removal of MB also increased from 95.6 to 97.2%. The adsorption capacity drastically drops from 71.7 to 36.5 mg g^{-1}. As the adsorbent increased from 0.02 to 0.05 g, percentage removal (% Removal) is already stabilised between 97.2% and 97.7% and goes to its maximum removal of 97.9% before slightly dropping to 97.8% at its maximum dosage. An increase in the removal percentage with increasing dosage is only significant between 0.01 to 0.02 g; this happens due to the large amount of bare surface area on the adsorption surface that can accommodate more MB molecules attached to the active site [19]. The availability of adsorption sites on bio-sorbent surfaces will increase the percentage of MB that will be removed from the solution. Further increment of XNL dosage above 0.02 g does not display a significant effect. Meanwhile, for the adsorption capacity, in contra, the adsorption capacity continually drops to 24.4 mg g^{-1} at 0.03 g, then 18.4 mg g^{-1} at 0.04 g, and finally drops to the lowest of 14.7 mg g^{-1} for 0.05 g. This phenomenon can be explained by the fact that at higher dosages, plenty of un-adsorbed adsorption sites on bio-sorbent surfaces happened and thus increased the ratio of the number of adsorption sites to the number of MB ions. This condition reduced the amount of MB adsorbed [20]–[22]. Deng et al. 2011 explained the reason for low adsorption capacity, which was due to the adsorption competition among the absorbent and also because of the splitting effect of concentration gradient, which is called flux. Another reason is due to the particle interaction of high adsorbent gradient, such as aggregation, which results from high bio-sorbent concentration. Due to this reason, the dosage of 0.02 g was chosen as an optimum dosage for further investigation.

Effect of MB Solution pH

The effect of the pH solution on the adsorption of MB onto XNL was performed by varying the pH of the MB solution between 2.0 and 10.0, as shown in Figure 3b. The lowest value of MB adsorption was recorded at pH 2 and increased to the highest amount of MB adsorbed at pH 10, but the increment of adsorption capacity was not significant, which increased only 49.79 mg g^{-1} (pH 5) to 50.07 mg g^{-1} (pH 10). Low adsorption at lower pH is due to competition of cationic dye with hydronium ion, H_3O^+ presence in large amount. The presence of H_3O^+ ion dominated the adsorbent surface, creating a strong repulsive force on cationic MB and consequently resulting in a decrease in MB uptake. Meanwhile, at pH 3 to pH 4, the amount of MB uptake increases sharply. This phenomenon can be explained by the deprotonated acidic hydrogen at a high pH value, making the adsorbent surface become negatively charged and creating an electrostatic potential between positively charged methylene blue (cationic dyes). In addition, the amount of H_3O^+ is slightly lower than pH 2, allowing more MB to be adsorbed onto the adsorbent surface. Since there is no significant increase in the amount of MB adsorbed onto the adsorbent at a pH higher than 6, the optimum pH condition chosen is pH 6. At this pH value, the adsorbent carries more negatively charged on the adsorbent surface since it is higher than the pH_{zpc} value (pH 5) and favourable for the adsorption of MB.

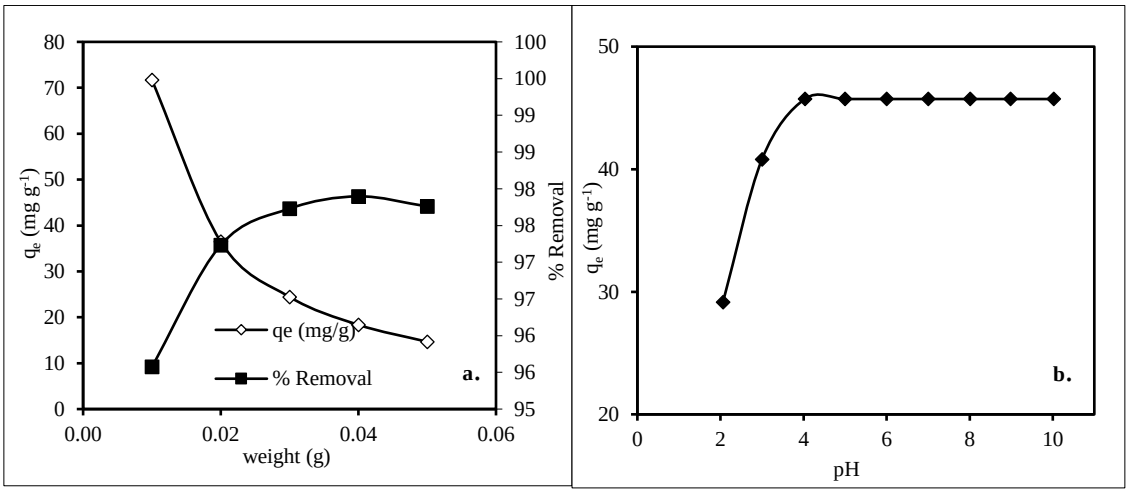

Figure 3 Effect of XNL dosage (a) and MB solution pH on adsorption of MB onto XNL.

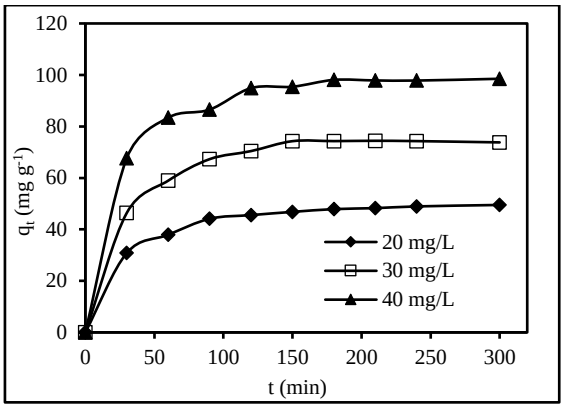

Figure 4 Effect of Initial Concentration and Contact Time Towards Adsorption of MB onto XNL.

Effect of MB Initial Concentration and Contact Time

The biosorption process was fast at the initial stage and gradually attained equilibrium, as shown in Figure 4. Rapid initial adsorption at the initial state recommended that there is a high affinity between MB dye and the functional group on the XNL surface. The time taken by MB to reach equilibrium onto XNL was 90 min for the initial concentration of 20 mg L^{-1} and 30 mg L^{-1}, but it took a much longer time, about 120 min for 40 mg L^{-1}, to reach equilibrium. After reaching equilibrium, the adsorption equilibrium q_t increases with an increase in initial MB concentration due to the significant driving forces generated by concentration gradient pressure [23] and also, the effective collision between MB and XNL surface is higher [3]. XNL recorded high q_t capacity. The q_t biosorption of MB onto XNL was 49.5 mg g^{-1} at 20 mg L^{-1}. With increased concentration to 30 mg L^{-1}, MB adsorbed q_t increases to 73.8 mg g^{-1}, while 40 mg L^{-1} gives the highest q_t of 98.5 mg g^{-1}. XNL showed good adsorption properties, suggesting that introducing a sulphur-bearing group onto raw adsorbent through xanthation can increase the adsorbent properties.

Adsorption Kinetic

The linear PFO and PSO kinetic models were applied to analyse the experimental data of the MB adsorption on XNL at different initial MB concentrations. The equations of the kinetic models PFO [24] and PSO [25] are expressed in Eqs. (3) and (4) respectively as follows:

$$\log(q_e - q_t) = \log q_e - \frac{k_1}{2.303}\, t \qquad (3)$$

$$\frac{t}{q_t} = \frac{1}{h} + \frac{1}{q_e}\, t \qquad (4)$$

where q_t (mg g^{-1}) and q_e (mg g^{-1}) are the amount of adsorbate adsorbed at time t (min) and at equilibrium, respectively, k_1 (min^{-1}) is a PFO rate constant. h (mg g^{-1} min^{-1}) is the initial adsorption rate that can be calculated as $h = k_2 q_e^2$. Meanwhile, k_2 (g $mg^{-1} min^{-1}$) is the PSO rate constant. The parameters of kinetic models were recorded in Table 2. According to experimental data (Table 2), it can be concluded that the adsorption of MB dye molecules by the XNL adsorbent follows the PSO model due to the higher correlation coefficient (R^2) values and the calculated q_e ($q_{e,cal}$) values fitted well with the experimental q_e ($q_{e,exp}$) values. This result suggests that the rate-determining step in the adsorption of MB onto XNL might be chemisorption involving valence forces through sharing or exchanging the valence electron of MB and the active surface of the XNL.

Table 2. PFO and PSO Kinetic Parameter for Adsorption of MB onto XNL.

	Pseudo First Order				Pseudo Second Order			
Initial Conc. (mg L^{-1})	**$q_{e,exp}$ (mg g^{-1})**	**$q_{e,cal}$ (mg g^{-1})**	**k_1 (min^{-1})**	**R^2**	**$q_{e,cal}$ (mg g^{-1})**	**h**	**k_2 (g mg^{-1} min^{-1})**	**R^2**
20	49.50	27.45	0.016	0.987	51.28	3.782	0.001	0.996
30	73.80	101.70	0.031	0.957	78.13	6.361	0.001	0.997
40	98.52	53.52	0.024	0.901	102.04	10.460	0.001	0.998

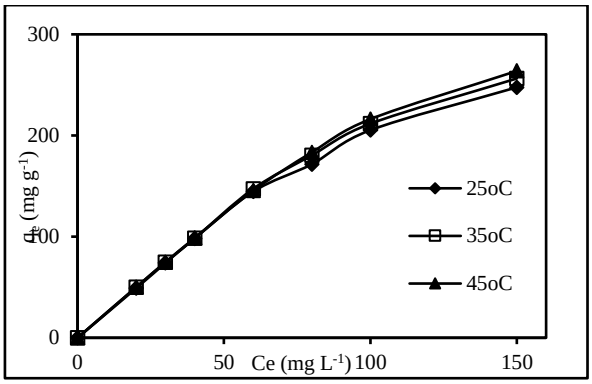

Figure 5. General Isotherm Plot for Adsorption of MB onto XNL

Effect of Temperature and Adsorption Isotherm

Based on the general isotherm plot (Figure 5), the adsorption capacity increased with temperature increase from 247.63 to 263.80 (mg g^{-1}), which suggests that the adsorption process is an endothermic process that requires energy [26].

Isotherm data of the MB-XNL system was further analysed using three isotherm models: Langmuir, Freundlich, and Dubinin-Reduskevich, which were utilised to fit the experimental data. The linear equations of the equilibrium models Langmuir [27], Freundlich [28], and Dubinin-Reduskevich [29] are presented in Eqs. (5), (6), and (7), respectively.

$$q_e = \frac{q_{max} b\, C_e}{(1+bC_e)} \quad (5)$$

$$q_e = K_f C_e^{1/n} \quad (6)$$

$$ln\, q_e = ln\, q_m - \beta\varepsilon^2 \quad (7)$$

Where C_e (mg L^{-1}) is the equilibrium concentration of adsorbate in the bulk solution, q_e (mg g^{-1}) is the amount of adsorbed adsorbate, q_{max} (mg g^{-1}) is the maximum adsorbate adsorbed and b (L mg^{-1}) is a Langmuir constant that related to the heat of adsorption. Where K_f (mg g^{-1}) is a constant that represents maximum adsorption capacity, and n is a parameter that relates to adsorption intensity. The plot of q_e vs log C_e will give 1/n while the intercept value is K_f. While ε (Polanyi potential) is equal to RT $\ln(1+1/C_e)$, R is the gas constant (8.314 J $mol^{-1}K^{-1}$), and T (K) is the temperature, q_m (mg g^{-1}) is the maximum adsorption capacity based on D-R isotherm and β is related to mean adsorption energy (E in kJ mol^{-1}) given by $E = \frac{1}{\sqrt{2\beta}}$. A plot of q_e vs ε^2 slope will be the value of β, while the intercept will give a value of maximum adsorption capacity, q_{max} (mg g^{-1}). The general isotherm plot for the adsorption of MB onto XNL is shown in Fig. 4.

The parameters of equilibrium models are recorded in Table 3. According to the R^2 values and adsorption capacity (Table 3) obtained from the isotherm models, it can be concluded that the adsorption process of MB dye on the surface of XNL follows Langmuir isotherm models. Moreover, this result also indicates that the MB dye adsorption occurred in monolayer [30]. The maximum monolayer adsorption capacity (q_{max}) of XNL for MB dye was recorded to be 263.80 mg g^{-1} at 318 K, which is 30 times higher than the un-treated adsorbent obtained by [31], which is 8.76 mg g^{-1}. Freundlich constant suggested that biosorption of MB onto XNL did not fit well with the Freundlich model, or in other words, the biosorption did not follow the assumption based on multilayer biosorption with heterogenous energetic distribution on the active surface sites. The temperature has a great influence on the adsorption process. From the Dubinin-Reduskevich model, the value of ε and q_m in XNL show an increasing trend when temperature increased from 298 to 318 K. From the E value, mean energy for the XNL adsorption is more than 16 mol^{-1} (18.26 – 129.10 kJ mol^{-1}) which could be evident of other chemisorption mechanism playing some major role [32]. These results are very encouraging compared with other adsorbents for MB adsorption described in Table 4. In addition, the prepared adsorbents are cheap and easy to synthesise.

Table 3. Adsorption Isotherms Parameter for MB Adsorption onto XNL at Different Temperatures.

		Langmuir			Freundlich			Dubinin-Radushkevich			
T (K)	**Q_{exp} (mg g^{-1})**	**Q_{max} (mg g^{-1})**	**b (L/mg)**	**R^2**	**K_F (mg g^{-1})**	**n**	**R^2**	**Q_{max} (mg g^{-1})**	**K**	**E (kJ/mol)**	**R^2**
298	247.63	238.09	0.44	0.982	103.25	3.81	0.959	587.40	0.0015	18.26	0.956
308	256.35	243.90	0.43	0.985	122.60	4.26	0.934	554.35	0.0002	50.00	0.948
318	263.80	250.00	0.51	0.983	128.74	4.34	0.945	533.68	0.00003	129.10	0.946

Table 4. Comparison of Monolayer Adsorption of MB onto Various Adsorbents.

Adsorbents	Maximum Monolayer Adsorption Capacity (mg g^{-1})	References
Xanthate-treated neem leaves powder	250.00	This study
Activated lemon peels	208.64	[23]
Ficus carica bast-activated carbon	47.62	[8]
Salsola vermiculata	23	[33]
Pyrolyzed *Salsola vermiculata*	53	[33]
Graphene	153.85	[34]
Soursop	55.39	[35]
Black cumin-activated carbon	26.32	[3]
Marine seaweed: *Caulerpa racemosa var. cylindracea*	5.23	[36]
Ackee apple pods activated carbon	47.17	[37]
Treated sugarcane bagasse	112.87	[38]

Adsorption Mechanism

The surface of XNL has a potential adsorption site such as the alkoxy (RO-) and hydroxyl (-OH), n and π electron group. Based on that, the adsorption mechanism of MB dye on the XNL surface by different types of interactions. Since there are a few functional groups of MB, it could form n - π or π - π bonding with lignocellulosic bio-sorbent surfaces as discussed in the characterisation discussion. This mechanism also involves the electrostatic interaction between MB dye cations with negatively charged available on the XNL surface. The adsorption mechanism also includes H-bonding interactions that can occur between the H atom available on the surface of XNL and the N atom in the MB dye structure. Finally, n-π interaction comes from delocalization of the lone pair electron of O atoms into the π orbital of the dye aromatic rings. According to the above, it can be concluded that these interactions were effective in enhancing the adsorption process of MB dye on the surface of XNL.

CONCLUSION

Xanthate-treated BNL powder successfully improved the performance of BNL by introducing a sulfur-containing group into the bio-sorbent. FTIR analysis proved the presence of the C-S bond, C=S stretching and C-O-C stretching. XNL was successfully approved can enhance the adsorption capacity of MB dye from an aqueous environment. The optimum adsorption conditions of MB dye onto the surface of XNL were determined to be 0.02 g XNL in 50 mL MB solution with pH 6 and continuously stirred at 480 rpm at 298 K. The kinetics data revealed that the adsorption was mainly affected by chemical adsorption with the maximum Langmuir adsorption capacity of XNL being 263.80 mg g^{-1} at 318 K for MB dye which is much higher than un-treated neem leaves powder. This proved that each adsorbent-adsorbate system will behave differently. The adsorption mechanism included H-bonding interaction and n-π interaction. The adsorption results discovered that the XNL is an effective and low-cost natural adsorbent for the removal of cationic dyes.

REFERENCE

1. Aichour, A., Zaghouane-Boudiaf, H., Iborra, C. V. & Polo, M. S. (2018) Bioadsorbent beads prepared from activated biomass/alginate for enhanced removal of cationic dye from water medium: Kinetics, equilibrium and thermodynamic studies. *Journal of Molecular Liquids*, **256**, 533–540. https://doi.org/10.1016/j.molliq.2018.02.073

2. Balistrieri, L. S. & Murray, J. W. (1981) The Surface Chemistry of Goethite (a-FeOOH) in Major Ion Seawater. *American Journal of Science*, 788–806, June 1981. https://doi.org/10.2475/ajs.281.6.788

3. Batool, F., Akbar, J., Iqbal, S., Noreen, S. & Bukhari, S. N. A. (2018) Study of Isothermal, Kinetic, and Thermodynamic Parameters for Adsorption of Cadmium: An Overview of Linear and Nonlinear Approach and Error Analysis. *Bioinorganic Chemistry and Applications*, *2018*. https://doi.org/10.1155/2018/3463724

4. Bello, M. O., Abdus-Salam, N., Adekola, F. A. & Pal, U. (2021) Isotherm and kinetic studies of adsorption of methylene blue using activated carbon from ackee apple pods. *Chemical Data Collections*, **31**. https://doi.org/10.1016/j.cdc.2020.100607

5. Bestani, B., Benderdouche, N., Benstaali, B., Belhakem, M. & Addou, A. (2008) Methylene blue and iodine adsorption onto an activated desert plant. *Bioresource Technology*, **99(17)**, 8441–8444. https://doi.org/10.1016/j.biortech.2008.02.053

6. Bhattacharya, K. G. & Sharma, A. (2005) Kinetics and thermodynamics of Methylene Blue adsorption on Neem (Azadirachta indica) leaf powder. *Dyes and Pigments*, **65(1)**, 51–59. https://doi.org/10.1016/j.dyepig.2004.06.016

7. Cengiz, S. & Cavas, L. (2008) Removal of methylene blue by invasive marine seaweed: Caulerpa racemosa var. cylindracea. *Bioresource Technology*, **99(7)**, 2357–2363. https://doi.org/10.1016/j.biortech.2007.05.011

8. Deng, H., Lu, J., Li, G., Zhang, G. & Wang, X. (2011) Adsorption of methylene blue on adsorbent materials produced from cotton stalk. *Chemical Engineering Journal*, **172(1)**, 326–334. https://doi.org/10.1016/j.cej.2011.06.013

9. Dubinin, M. ., Zaverina, E. & Radushkevich, L. (1947) Sorption and structure of active carbons. I. Adsorption of organic vapors. *Journal of Physical Chemistry*, **21**, 1531–1362.

10. Fomina, M. & Gadd, G. M. (2014) Biosorption: Current perspectives on concept, definition and application. *Bioresource Technology*, **160**, 3–14. https://doi.org/10.1016/j.biortech.2013.12.102

11. Freundlich, H. (1906) Adsorption in solutions. *Journal of Physical Chemistry*, **57**, 385–470.

12. Gao, G., Zhou, P., Chen, C. & Zhu, L. (2023) Adsorption of MB and Pb (II) before and after magnetic modification : Performance and mechanism. *Journal of Molecular Structure Journal*, **1293**, July, 2023. https://doi.org/https://doi.org/10.1016/j.molstruc.2023.136306

13. Gobi, K., Mashitah, M. D. & Vadivelu, V. M. (2011) Adsorptive removal of Methylene Blue using novel adsorbent from palm oil mill effluent waste activated sludge: Equilibrium, thermodynamics and kinetic studies. *Chemical Engineering Journal*, **171(3)**, 1246–1252. https://doi.org/10.1016/j.cej.2011.05.036

14. Ho, Y. (2000) The kinetics of sorption of divalent metal ions onto sphagnum moss peat. *Water Research*, **34(3)**, 735–742. https://doi.org/10.1016/S0043-1354(99)00232-8

15. Ho, Y. S. & McKay, G. (1998) A Comparison of Chemisorption Kinetic Models Applied to Pollutant Removal on Various Sorbents. *Process Safety and Environmental Protection*, **76(4)**, 332–340. https://doi.org/10.1205/095758298529696

16. Islas, J. F., Acosta, E., G-buentello, Z., Delgado-gallegos, J. L., Autónoma, U., León, D. N., Medicina, F. De, Bioquímica, D. De, Francisco, A., Madero, I. & Pequeño, A. (2020) An overview of Neem (Azadirachta indica) and its potential impact on health. *Journal of Functional Foods*, **74**, 104171, April, 2020. https://doi.org/10.1016/j.jff.2020.104171

17. Ismail, M. & Hanafiah, K. M. (2020) Kinetic, isotherm, and possible mechanism of Pb(II) ion adsorption onto xanthate neem (Azadirachta indica) leaf powder. *Sains Malaysiana*, **49(7)**. https://doi.org/10.17576/jsm-2020-4907-11

18. Kumar, A., Rao, N. N. & Kaul, S. N. (2000) Alkali-treated straw and insoluble straw xanthate as low-cost adsorbents for heavy metal removal - preparation, characterization and application. *Bioresource Technology*, **71(2)**, 133–142. https://doi.org/10.1016/S0960-8524(99)00064-4

19. Langmuir, I. (1916) The Constitution and Fundamental Properties of Solids and Liquids. Part 1. Solids. *Journal of the American Chemical Society*, **38(11)**, 2221–2295. https://doi.org/10.1021/ja02268a002

20. Liu, T., Li, Y., Du, Q., Sun, J., Jiao, Y., Yang, G., Wang, Z., Xia, Y., Zhang, W., Wang, K., Zhu, H. & Wu, D. (2012) Adsorption of methylene blue from aqueous solution by graphene. *Colloids and Surfaces B: Biointerfaces*, **90(1)**, 197–203. https://doi.org/10.1016/j.colsurfb.2011.10.019

21. Manjunatha, K. R. & Vagish, M. (2016) Study on Adsorption Efficiency of Neem Leaves Powder in Removal of Reactive Dye Color from Aqueous Solution. *International Research Journal of Engineering and Technology*, **3(7)**, 437–440.

22. Maysl, T. J. (2007) A new classification of pore sizes. In *Studies in Surface Science and Catalysis, Issue 0, Elsevier B.V.*, **160**. https://doi.org/10.1016/S0167-2991(07)80009-7

23. Meili, L., Lins, P. V. S., Costa, M. T., Almeida, R. L., Abud, A. K. S., Soletti, J. I., Dotto, G. L., Tanabe, E. H., Sellaoui, L., Carvalho, S. H. V. & Erto, A. (2019) Adsorption of methylene blue on agroindustrial wastes: Experimental investigation and phenomenological modelling. *Progress in Biophysics and Molecular Biology*, **141**, 60–71. https://doi.org/10.1016/j.pbiomolbio.2018.07.011

24. Momčilović, M., Purenović, M., Bojić, A., Zarubica, A. & Randelovid, M. (2011) Removal of lead(II) ions from aqueous solutions by adsorption onto pine cone-activated carbon. *Desalination*, **276(1–3)**, 53–59. https://doi.org/10.1016/j.desal.2011.03.013

25. Nasuha, N., Hameed, B. H. & Din, A. T. M. (2010) Rejected tea as a potential low-cost adsorbent for the removal of methylene blue. *Journal of Hazardous Materials*, **175(1–3)**, 126–132. https://doi.org/10.1016/j.jhazmat.2009.09.138

26. Oladoye, P. O., Ajiboye, T. O., Omotola, E. O. & Oyewola, O. J. (2022) Methylene blue dye: Toxicity and potential elimination technology from wastewater. *Results in Engineering*, **16**, 100678, August, 2022. https://doi.org/10.1016/j.rineng.2022.100678

27. Pathania, D., Sharma, S. & Singh, P. (2017) Removal of methylene blue by adsorption onto activated carbon developed from Ficus carica bast. *Arabian Journal of Chemistry*, **10**, S1445–S1451. https://doi.org/10.1016/j.arabjc.2013.04.021

28. Ramsay, R. R., Dunford, C. & Gillman, P. K. (2007) Methylene blue and serotonin toxicity: inhibition of monoamine oxidase A (MAO A) confirms a theoretical prediction. *British Journal of Pharmacology*, **152(6)**, 946–951. https://doi.org/10.1038/sj.bjp.0707430

29. Rasheed, A., Danish, M., Gulfam, M., Majeed, S. & Alanazi, A. M. (2024) A review of pre- and post-surface-modified neem (Azadirachta indica) biomass adsorbent : Surface functionalization mechanism and application. *Chemosphere*, **351**, 141180, September 2023. https://doi.org/10.1016/j.chemosphere.2024.141180

30. Sadare, O. O., Ayeni, A. O. & Daramola, M. O. (2022) Evaluation of adsorption and kinetics of neem leaf powder (Azadirachta indica) as a bio-sorbent for desulfurization of dibenzothiophene (DBT) from synthetic diesel. *Journal of Saudi Chemical Society*, **26(2)**. https://doi.org/10.1016/j.jscs.2022.101433

31. Salah Omer, A., El Naeem, G. A., Abd-Elhamid, A. I., Farahat, O. O. M., El-Bardan, A. A., Soliman, H. M. A. & Nayl, A. A. (2022) Adsorption of crystal violet and methylene blue dyes using a cellulose-based adsorbent from sugarcane bagasse: characterization, kinetic and isotherm studies. *Journal of Materials Research and Technology*, **19**, 3241–3254. https://doi.org/10.1016/j.jmrt.2022.06.045

32. Senthilkumaar, S., Varadarajan, P. R., Porkodi, K. & Subbhuraam, C. V. (2005) Adsorption of methylene blue onto jute fibre carbon: Kinetics and equilibrium studies. *Journal of Colloid and Interface Science*, **284(1)**, 78–82. https://doi.org/10.1016/j.jcis.2004.09.027

33. Subhan, F., Aslam, S., Yan, Z., Yaseen, M., Naeem, M., Ikram, M., Ali, A. & Bibi, S. (2022) Adsorption and reusability performance of hierarchically porous silica (MMZ) for the removal of MB dye from water. *Inorganic Chemistry Communications*, **139**, 109380, March, 2022. https://doi.org/10.1016/j.inoche.2022.109380

34. Thabede, P. M., Shooto, N. D. & Naidoo, E. B. (2020) Removal of methylene blue dye and lead ions from aqueous solution using activated carbon from black cumin seeds. *South African Journal of Chemical Engineering*, **33**, 39–50. https://doi.org/10.1016/j.sajce.2020.04.002

35. Torres-Blancas, T., Roa-Morales, G., Fall, C., Barrera-Díaz, C., Ureña-Nuñez, F. & Pavón Silva, T. B. (2013) Improving lead sorption through chemical modification of de-oiled allspice husk by xanthate. *Fuel*, **110**, 4–11. https://doi.org/10.1016/j.fuel.2012.11.013

36. Yaashikaa, P. R., Kumar, P. S., Saravanan, A. & Vo, D. N. (2021) Advances in biosorbents for removal of environmental pollutants : A review on pretreatment, removal mechanism and future outlook. *Journal of Hazardous Materials*, **420**, 126596, June, 2021. https://doi.org/10.1016/j.jhazmat.2021.126596

37. Zhang, W., Yan, H., Li, H., Jiang, Z., Dong, L., Kan, X., Yang, H., Li, A. & Cheng, R. (2011) Removal of dyes from aqueous solutions by straw-based adsorbents: Batch and column studies. *Chemical Engineering Journal*, **168(3)**, 1120–1127. https://doi.org/10.1016/j.cej.2011.01.094